Reconstructing the upper water column thermal structure in the Atlantic Ocean

Caroline Cléroux,[1,2] Peter deMenocal,[1] Jennifer Arbuszewski,[1,3] and Brad Linsley[1]

Received 21 January 2013; revised 29 August 2013; accepted 30 August 2013.

[1] The thermal structure of the upper ocean (0–1000 m) is set by surface heat fluxes, shallow wind-driven circulation, and the deeper thermohaline circulation. Its long-term variability can be reconstructed using deep-dwelling planktonic foraminifera that record subsurface conditions. Here we used six species (*Neogloboquadrina dutertrei*, *Globorotalia tumida*, *Globorotalia inflata*, *Globorotalia truncatulinoides*, *Globorotalia hirsuta*, and *Globorotalia crassaformis*) from 66 core tops along a meridional transect spanning the mid-Atlantic (42°N to 25°S) to develop a method for reconstructing past thermocline conditions. We estimated the calcification depths from $\delta^{18}O$ measurements and the Mg/Ca-temperature relationships for each species. This systematic strategy over this large latitudinal section reveals distinct populations with different Mg/Ca-temperature relationships for *G. inflata*, *G. truncatulinoides*, and *G. hirsuta* in different areas. The calcification depths do not differ among the different populations, except for *G. hirsuta*, where the northern population calcifies much shallower than the southern population. *N. dutertrei* and *G. tumida* show a remarkably constant calcification depth independent of oceanographic conditions. The deepest dweller, *G. crassaformis*, apparently calcifies in the oxygen-depleted zone, where it may find refuge from predators and abundant aggregated matter to feed on. We found a good match between its calcification depth and the 3.2 ml/l oxygen level. The results of this multispecies, multiproxy study can now be applied down-core to facilitate the reconstruction of open-ocean thermocline changes in the past.

Citation: Cléroux, C., P. deMenocal, J. Arbuszewski, and B. Linsley (2013), Reconstructing the upper water column thermal structure in the Atlantic Ocean, *Paleoceanography*, *28*, doi:10.1002/palo.20050.

1. Introduction

[2] Recent decades of oceanographic research have highlighted the structure of the subsurface ocean and its regional and global climate impacts. More than 30% of the ocean poleward heat transport is accomplished within the upper ocean [*Boccaletti et al*., 2005], which interacts with the atmosphere [*Willis et al*., 2004]. Temperature and salinity changes observed between 300 and 1000 m depth over the last several decades have brought into focus the lack of understanding in long-term variability of the subsurface conditions and the connection to large-scale circulation [*Levitus et al*., 2000; *Lozier et al*., 2008].

[3] As shown from pioneering field observations [*Bé and Tolderlund*, 1971; *Fairbanks and Wiebe*, 1980] and isotope studies [*Bé et al*., 1977; *Deuser and Ross*, 1989; *Fairbanks et al*., 1980], deep-dwelling planktonic foraminifera, those living in the upper few hundred meters of the water column, can provide such archives for past subsurface conditions. Stable oxygen isotopes ($\delta^{18}O$) of planktonic foraminifera shell have previously been used to constrain the calcification depth for deep-dwelling species [*Fairbanks et al*., 1980; *Farmer et al*., 2007; *Steph et al*., 2009]. Shell $\delta^{18}O$ indicates a much smaller depth range than the vertical migration range suggested from field observational studies [*Fairbanks et al*., 1980; *Schiebel and Hemleben*, 2005]; the calcification depths deduced from shell $\delta^{18}O$ are therefore the mean depths where the shells calcify and record ambient conditions. More recently, the search for subsurface temperature proxies has led to the development of Mg/Ca-temperature relationships for deep-dwelling planktonic foraminifera [*Anand et al*., 2003]. These relationships between Mg/Ca and temperature are species and basin specific and are also sensitive to sample treatment [*Barker et al*., 2005]. Despite these previous efforts, only a limited number of studies have investigated the calcification depth of deep-dwelling species over broad geographical areas [*Ganssen and Kroon*, 2000; *Mulitza et al*., 1997], and previous Mg/Ca-temperature calibrations are insufficient to cover the full spectrum of species, oceanographic

Additional supporting information may be found in the online version of this article.

[1]Lamont-Doherty Earth Observatory, Columbia University, Palisades, New York, USA.

[2]Now at Department of Marine Geology, NIOZ Royal Netherlands Institute for Sea Research, Den Burg, Netherlands.

[3]Now at Woods Hole Oceanographic Institution, Woods Hole, Massachusetts, USA.

Corresponding author: C. Cléroux, Department of Marine Geology, NIOZ Royal Netherlands Institute for Sea Research, Landsdiep 4, Den Burg, 1797, Netherlands. (Caroline.Cleroux@nioz.nl)

0883-8305/13/10.1002/palo.20050

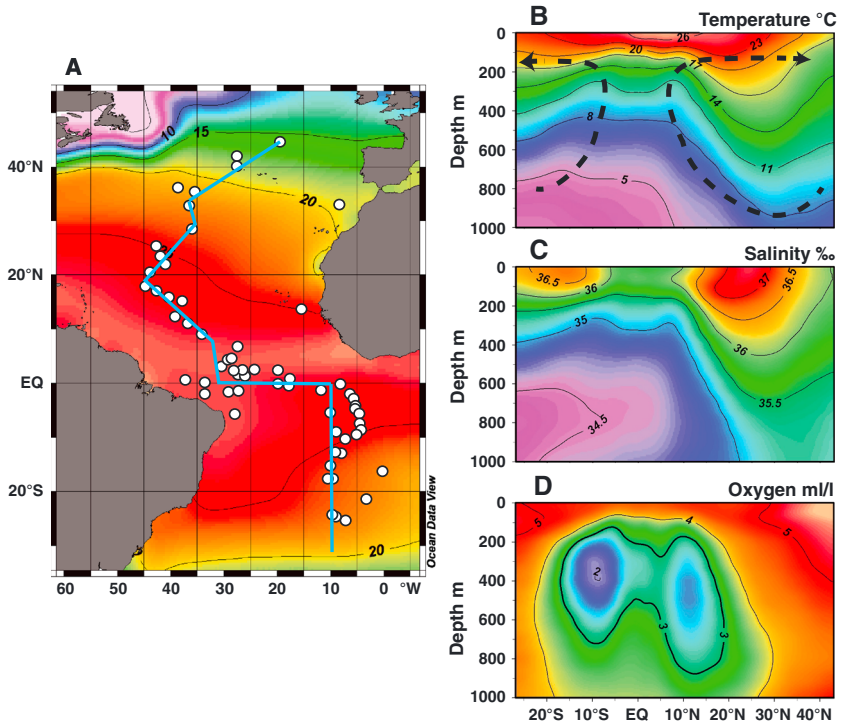

Figure 1. Sea surface temperature map showing the (a) location of the core-top samples and the (b) temperature, (c) salinity, and (d) oxygen sections versus latitude following the core-top transect (blue line in Figure 1a) for the upper 1000 m depth. Arrows in Figure 1b illustrate the vertical circulation (STC).

context, and cleaning procedure [*Cléroux et al.*, 2008; *Groeneveld and Chiessi*, 2011; *Regenberg et al.*, 2009].

[4] In this study, we build on these previous results to establish proxies for thermocline conditions in the Atlantic Ocean. We analyzed the $\delta^{18}O$ and Mg/Ca compositions of six deep-dwelling planktonic foraminifera species, one from the neogloboquadrinid genus (*Neogloboquadrina dutertrei*) and five from the globorotaliid genus (*Globorotalia tumida*, *Globorotalia inflata*, *Globorotalia truncatulinoides*, *Globorotalia hirsuta* and *Globorotalia crassaformis*). We also use previously published data for the surface dweller foraminifera (*Globigerinoides ruber* white) [*Arbuszewski et al.*, 2010]. A unique feature of this study is the large latitudinal gradient (42°N to 25°S) covered by the core-top samples spanning a variety of oceanographic regimes in the Atlantic Ocean. This large transect crosses regions potentially associated with distinctive genetic foraminiferal species populations [*Darling et al.*, 2006; *Morard et al.*, 2011; *Quillévéré et al.*, 2013], and one objective is to look at the geochemical response of the same morphometric species within different ecological niches. Along our core-top transect, the isotherms and isohalines (and therefore iso-$\delta^{18}O$ lines) present drastic depth changes (up to 450 m) in response to the subsurface circulation. Down to about 400 m depth, the subsurface circulation in this tropical/subtropical region is described by shallow meridional overturning circulation connecting the midlatitudes and the tropics, called the subtropical cells (STC) [*Liu and Yang*, 2003]. Below the STC, the subsurface Atlantic Ocean is influenced by the return flow of the thermohaline circulation with the fresh Sub-Antarctic Mode Water flowing from the South Atlantic between 400 and 1000 m. STC and southern-sourced mode water create temperature and salinity isotherm structures ideal to determine the calcification depth of deep-dwelling planktonic species under different conditions.

[5] This paper is organized as follows. In the first part we determine the mean calcification depth as recorded by the mean $\delta^{18}O$ of the foraminifer tests. In the second part we calibrate the paired Mg/Ca ratio measurements with the isotopic temperature. In the final section we combine the deduced calcification depth, the Mg/Ca ratio, and all ocean parameters available to characterize each species calcification habitat and identify separate subpopulations for three of the deep-dwelling foraminifera species.

2. Oceanographic Context

[6] We selected 66 core tops between 42°N and 25°S in the Atlantic Ocean, mostly located along the flanks of the mid-Atlantic ridge (Figure 1a). The sea surface temperature and salinity fields over this region reflect the mean position of the Intertropical Convergence Zone (ITCZ) and the evaporation/precipitation balance over the Atlantic Ocean. Maximum temperature and minimum salinity around 5°N separate the two warm and salty subtropical gyres. These structures are visible on the vertical temperature and salinity profiles down to about 200 m depth (Figures 1b and 1c). At greater depth the subsurface circulation, i.e., the subtropical cells (STC), and the return flow of the thermohaline circulation determine the structures of the isotherms and isohalines. In both subtropical gyres, water in the salinity maximum is subducted in winter by Ekman forcing and circulates toward the equator within the thermocline [*Liu and Alexander*, 2007]. Following either the western boundary or interior

Table 1. Core-Top Locations, Depths, Sample Levels, and Stratigraphic Constraints[a]

Sample ID	Latitude °N	Longitude °W	Depth (m)	Sample Depth (cm)	Stratigraphy	^{14}C Ages	Calibrated Ages
VM29-178	42.85	−25.15	3448	6.5	iso. Strat. + 14C	6.5 cm = 3775 ± 30[b]	3719 ± 101
VM30-97	41.00	−32.93	3371	5.5	14C	5.5 cm = 5030 ± 35[b]	5379 ± 87
VM30-96	39.95	−33.13	3188	3.5	14C	3.5 cm = 6005 ± 30[b]	6407 ± 93
VM27-267	35.63	−44.28	4722	0	14C	0 cm = 3495 ± 35[b]	3376 ± 93
VM27-263	35.02	−40.92	3704	9.5	14C	9.5 cm = 6440 ± 30[b]	6926.5 ± 107
VM27-161	33.58	−13.97	4446	0	14C	0 cm = 4550 ± 35[b]	4737 ± 103
VM17-165	32.75	−41.90	3924	4	iso. Strat.		
VM19-308	29.02	−41.40	3197	4.5	14C	4.5 cm = 4520 ± 35[b]	4711.5 ± 111
VM20-244	26.00	−48.27	3953	1.5	iso. Strat.		
VM10-93	24.20	−47.47	3574	2.5	iso. Strat.		
VM16-206	23.33	−46.48	3733	6.5	iso. Strat.		
VM14-2	20.72	−49.43	4171	2.5	iso. Strat.		
VM16-20	17.93	−50.35	4539	3.5	iso. Strat.		
VM16-21	17.27	−48.42	3975	3.5	14C	7.5 cm = 7800 ± 200[c]	8289 ± 452
VM16-22	16.40	−45.77	3948	0.5	iso. Strat.		
VM16-205	15.40	−43.40	4043	6.5	iso. Strat.		
VM22-202	14.40	−21.15	4310	0	% carbonate		
VM25-44	11.50	−45.15	4049	2.5	iso. Strat.		
VM32-67	11.28	−42.50	4082	2.5	14C	4.5 cm = 3420 ± 70[d]	3276 ± 180
VM16-203	9.35	−39.87	4158	1.5	% carbonate		
VM20-234	5.32	−33.03	3133	9.5	iso. Strat. + 14C	13.5 cm = 5395 ± 30[b]	5772 ± 99
VM25-60	3.30	−34.80	3749	3.5	iso. Strat. + 14C	10 cm = 4750 ± 190[c]	4995 ± 484
VM22-30	3.25	−34.25	3529	7.5	iso. Strat.		
VM20-233	2.01	−35.93	3884	4.5	Glamap		
RC13-189	1.85	−30.00	3233	4.5	iso.Strat.		
VM22-31	1.85	−32.47	3436	7.5	% coarse fraction		
RC13-188	1.80	−33.70	3451	3			
RC13-190	1.78	−25.43	3797	0	iso. Strat. + 14C	0.5 cm = 3600 ± 30[b]	3491 ± 94
VM25-59	1.37	−33.48	3824	2.5	iso. Strat. + 14C	15 cm = 5785 ± 35[e]	4252 ± 81
VM22-32	0.90	−31.80	2999	6			
VM14-5	0.85	−32.85	3255	8	Glamap		
RC24-01	0.55	−13.65	3837	0	Mix et al 1986		
RC24-02	0.55	−13.68	3880	0	iso. Strat. + 14C	12 cm = 5880 ± 30[e]	6303 ± 78
VM30-41	0.22	−23.07	3874	1.5	iso. Strat. + 14C	3.5 cm = 1700 ± 120[c]	1248 ± 258
VM25-50	0.20	−42.77	3749	5.5	CLIMAP		
VM27-181	0.07	−25.48	3601	4.5	% carbonate		
VM30-40	−0.20	−23.15	3706	0	iso. Strat. + 14C	5 cm = 2410 ± 170[c]	2046 ± 429
VM26-102	−0.38	−39.13	4301	0	menardii		
VM22-182	−0.53	−17.27	3614	9.5	iso. Strat.		
RC24-07	−1.34	−11.90	3899	0	iso. Strat.		
RC24-08	−1.33	−11.90	3882	2.5	iso. Strat. + 14C	2.5 cm = 3770 ± 30[f]	3783 ± 100
VM26-99	−1.47	−32.72	4632	0	% carbonate		
VM26-100	−1.55	−34.65	4308	0	Mix et al, 1999		
VM20-230	−1.95	−39.03	3294	3	Glamap		
RC24-11	−2.18	−11.25	3445	0	iso. Strat. + 14C	0.5 cm = 2655 ± 35[e]	2364 ± 105
RC24-13	−3.73	−10.88	3921	0	% carbonate		
RC24-15TWT	−4.10	−10.87	3504	0	% carbonate		
VM22-179	−4.88	−15.73	3576	2.5	Glamap		
RC24-16TWT	−5.03	−10.18	3559	0	iso. Strat.		
RC24-17	−5.05	−10.18	3559	0.5	iso. Strat. + 14C	0 cm = 2635 ± 35[e]	2315 ± 119
RC11-17	−5.28	−33.43	4490	0			
RC24-19TWT	−7.02	−10.00	3581	0	iso. Strat.		
RC24-21TWT	−8.18	−10.12	3718	0			
VM22-175	−8.77	−14.28	2950	1.5	% carb. + menardii		
RC13-210	−9.13	−10.60	3658	7.5	% carb. + menardii		
VM22-174	−10.07	−12.82	2630	1.5	iso. Strat. + 14C	16.8 cm = 7365 ± 30[c]	7844 ± 579
INMD111	−12.64	−13.85	3069	0.5	iso. Strat. + 14C	1 cm = 3940 ± 90[g]	3932 ± 254
RC16-77	−12.70	−13.40	3404	6.5	iso. Strat		
INMD113	−15.26	−14.96	3471	1.5	iso. Strat. + 14C	1 cm = 4895 ± 85[g]	5196 ± 242
VM22-169	−16.25	−5.73	3499	3.5	Glamap		
INMD115	−17.64	−16.21	3427	1.5	iso. Strat. + 14C	1 cm = 4850 ± 165[g]	5170 ± 399
VM16-35	−17.65	−15.10	3891	7.5	% carbonate		
VM16-37	−21.33	−8.95	3908	3.5	iso. Strat.		
RC8-18	−24.07	−15.12	3977	6.5			
RC8-19	−24.30	−14.70	3636	10.5	% carbonate		
RC8-23	−25.15	−12.77	3338	9.5	iso. Strat.		

[a]The stratigraphy column gives the nature of the stratigraphic control. Some samples have already been presented in previous studies: Climate: Long-Range Investigation, Mapping, and Prediction (CLIMAP), GLODAP, [*Mix*, 1986], or [*Mix et al*., 1999]. Otherwise, isotopic stratigraphy, *Globorotalia menardii* abundance [*Ericson and Wollin*, 1968], and/or carbonate content were used for stratigraphic constraint; most of the data are on the Pangaea database. Five core tops are lacking any age control. Signs in the ^{14}C data column give the reference. ^{14}C ages were calibrated to calendar ages using Calib6 and the conventional reservoir age of 400 years [*Reimer et al*., 2009].

[b]This study.

[c]CLIMAP.

[d]*Broecker et al*. [1993].

[e]*Arbuszewski et al*. [2010].

[f]*Cléroux et al*. [2011].

[g][*Berger et al*., 1985].

Table 2. Mean T_{iso} and Values Used to Calculate the Error on T_{iso} for Each Species

Species	Mean T_{iso} (δ^{18}Osw Taken at the Calcification Depth)	Mean T_{iso} (Fixed δ^{18}Osw Value)	Error on δ^{18}Osw	Mean SD of $\delta^{18}O_{foram}$ Replicate	Error on T_{iso}
N. dutertrei	17.9°C	18.04°C (0.7‰)	0.15°C	0.16‰	0.66°C
G. crassaformis	6.1°C	5.6°C (0‰)	0.5°C	0.15‰	0.78°C
G. hirsuta	9.12°C	8.8°C (0.3‰)	0.3°C	0.08‰	0.44°C
G. inflata	11.3°C	11.1°C (0.4‰)	0.2°C	0.09‰	0.41°C
G. truncatulinoides	10.0°C	9.9°C (0.3‰)	0.1°C	0.16‰	0.65°C
G. tumida	15.0°C	14.9°C (0.6‰)	0.1°C	0.14‰	0.57°C

routes, these water masses then reach the equatorial upwelling regions. At the equator, Ekman transport on the surface layers expels the upwelled water poleward, closing the STC loops (Figure 1b) [*Schott et al*., 2004; *Zhang et al*., 2003]. The role of the STC in communicating extratropical climate anomalies into the tropics was first observed in the Pacific Ocean [*Gu and Philander*, 1997]; such teleconnection process is now referred to as "oceanic tunnel" [*Liu and Alexander*, 2007]. The basin-wide meridional overturning circulation in the Atlantic Ocean, associated with North Atlantic deep water formation [*Fratantoni et al*., 2000] and the mean location of the ITCZ north of the equator, induces an asymmetry in the STC. The southern STC is stronger with a larger relative contribution of southern-sourced waters to the subsurface equatorial water mass [*Harper*, 2000; *Snowden and Molinari*, 2003]; as a consequence the temperature and salinity structure about the equator are asymmetric (Figure 1). Nutrient profiles across our section show the same pattern as the temperature and salinity sections (not shown).

[7] Oxygen content in the ocean is controlled both by large-scale water ventilation and biogeochemical cycles. Well-ventilated waters subducting into the thermocline at midlatitude are deflected toward the west, leaving a shadow zone of less ventilated water on the eastern margin. The central and eastern tropical Atlantic host an oxygen minimum zone, centralized around 400 m depth on both sides of the equator (Figure 1d).

[8] Beside these meridional structures, a complex system of surface and subsurface ocean currents operates in the equatorial region. It includes the eastward North Equatorial Countercurrent between 3°N and 10°N, flanked by the westward flowing North Equatorial Current and South Equatorial Current. Below the latter is the intense eastward Equatorial Undercurrent, located precisely at the equator at about 100 m depth. This system generates complex temperature and salinity fields. Plotting these parameters against latitude results in large temperature and salinity variability in the equatorial band (Figure S1 in supporting information); we will see that foraminifera record this variability remarkably well.

3. Material and Methods

3.1. Core-Top Selection

[9] We present 66 core tops from the tropical-subtropical Atlantic Ocean. Most of these samples are from the Lamont Core Repository, the details about which have been previously presented in *Arbuszewski et al*. [2010] together with the *G. ruber* (white) δ^{18}O and Mg/Ca data. We added three samples in the subtropical South Atlantic from the Scripps Core repository (INMD111, INMD113, and INMD115) to increase the coverage in the south Atlantic gyre. Most samples are located above the modern Atlantic lysocline (4000 m water depth). Various criteria ensure the Holocene age of the core tops; i.e., radiocarbon dating, oxygen isotope stratigraphies, *Globorotalia menardii* stratigraphies [*Ericson and Wollin*, 1968], down-core carbonate content, or down-core coarse fraction content (Table 1). As with any core-top study, a caveat to our approach is that a few samples may not be truly modern. We estimate, from the radiocarbon ages or isotopic stratigraphies, that at least half of our core-top samples are younger than 4 ka (although a few may be as old as 6 ka), which may contribute to some noise when comparing with modern atlas data.

3.2. Species Selection

[10] Species were selected according to three criteria: abundances in the samples, various habitat depths according to previous studies, and persistence during glacial times in the Atlantic Ocean. Many planktonic foraminifera species have a dextral and a sinistral form, depending on their coiling direction. The controlling parameters for this are not clear; the coiling direction can be associated or not with different genetic species [*de Vargas et al*., 2001]; it can correspond or not to different Mg/Ca to temperature relationships [*Cléroux et al*., 2008], and the dominant coiling form can change on spatial or temporal scales [*Ericson et al*., 1954]. For our study, we selected the most abundant coiling direction for each species throughout the entire sample set. *N. dutertrei*, *G. tumida*, *G. inflata*, *G. truncatulinoides* dextral, G. *hirsuta* dextral, and *G. crassaformis* sinistral were carefully picked from the 355–425 μm fraction. All specimens had thick and opaque walls. Between 10 and 25 specimens were picked, gently crushed between two glass plates, mixed, and split into four aliquots: two replicates for trace element analysis and two replicates for stable isotope analysis. In a limited number of samples, the foraminifer abundance was low, and only one measurement per analysis type was performed.

3.3. Isotope and Trace Element Measurements

[11] Prior to oxygen and carbon stable isotope analysis, samples were cleaned by several ultrapure water rinses and sonication. δ^{18}O and δ^{13}C analyses were made at State University of New York (SUNY) in Albany using a Fisons Optima mass spectrometer with dual-inlet and multiprep system calibrated with NBS19 and NBS18 standards. The long-term precision during the analysis period was <0.05‰ for δ^{18}O and <0.03‰ for δ^{13}C.

[12] Prior to trace element analysis, samples were cleaned with several ultrapure water and methanol washes followed by both the oxidative and the reductive step of the *Boyle and Keigwin* [1985] protocol. Samples were dissolved just before measurement on the Jobin-Yvon Panorama-V ICP-OES at

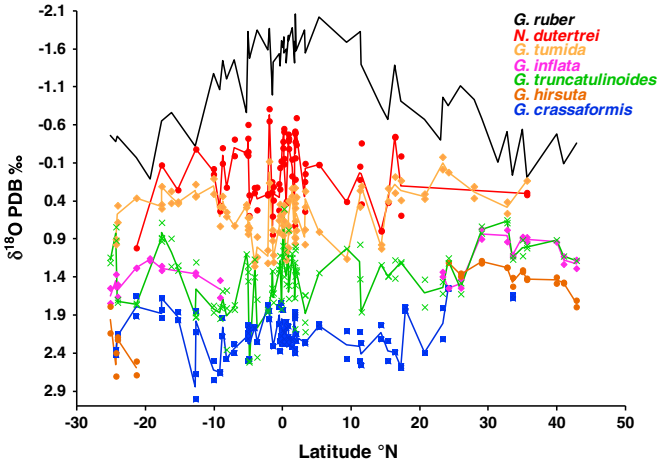

Figure 2. $\delta^{18}O$ results for all the species versus latitude. All the replicates are plotted, except for *G. ruber* data that come from *Arbuszewski et al.* [2010]; the thin, dark curves represent the mean value.

Lamont and calibrated with in-house standards. The long-term standard deviation of international standards (CM 1767, ECRM 752-1, and BAM RS3) are respectively 0.13, 0.05, and 0.06 mmol/mol for the solutions with Mg/Ca ratios of 5.73, 3.82, and 0.77 mmol/mol [*Greaves et al.*, 2008]. The absolute values of these standards measured during each run are always within a few percent of the published values (<3%).

3.4. Ocean Atlas Data

[13] At each core-top location and for the following depths, 0, 50, 100, 125, 150, 200, 300, 400, 500, 600, 700, 800, 900, and 1000 m, we extracted the mean annual temperature, salinity, oxygen concentration, and phosphate concentration from the World Ocean Atlas (WOA) 2009 [*Antonov et al.*, 2010; *Garcia et al.*, 2010a; *Garcia et al.*, 2010b; *Locarnini et al.*, 2010]. Below 100 m depth, seasonal temperature variations are typically around 1°C. One exception is the North Atlantic tropical region (9.51°N–1°N), where seasonal temperature variation at 100 m depth reaches 8°C. We could not identify any effect of the particularly large seasonality in this region on the foraminiferal data and therefore only used mean conditions for the rest of the study. Similarly, for the same locations and depths, we extracted seawater $\delta^{18}O$ ($\delta^{18}Osw$) values from the Goddard Institute for Space Studies database [*LeGrande and Schmidt*, 2006]. These modeled values take into account the various $\delta^{18}Osw$-salinity relationships and best represent measured $\delta^{18}Osw$ values [*Schmidt et al.*, 1999]. Finally, we used the Global Ocean Data Analysis Project (GLODAP) database for Total Alkalinity and Total CO_2 data, corrected for anthropogenic CO_2 [*Broecker et al.*, 2004]. At each core-top location and for each depth level, we calculated the pre-anthropogenic pH, the carbonate ion concentration [CO_3^{2-}], and bottom water carbonate saturation (ΔCO_3^{2-}) using the CO2sys software [*Lewis and Wallace*, 1998].

3.5. Calcification Depth Calculation

[14] The calcification depth for each sample is calculated by matching the foraminiferal $\delta^{18}O$ ($\delta^{18}O_{foram}$) with the $\delta^{18}O$ of calcite ($\delta^{18}O_{calc}$) calculated for known depths.

[15] Assuming equilibrium with seawater, we used the *Kim and O'Neil* [1997] equation (equation (1)).

$$\delta^{18}O_{calc} = 25.778 - 3.333 \times \sqrt{(43.704 + Temp)} + (\delta^{18}O_{sw} - 0.27) \quad (1)$$

[16] The $\delta^{18}Osw$, expressed on the SMOW scale, is converted to the Pee Dee Belemnite (PDB) scale by subtracting 0.27 [*Hut*, 1987]. Since the earliest work on this proxy [*Epstein et al.*, 1953], several $\delta^{18}O$-temperature equations have been developed. We chose the *Kim and O'Neil* [1997] equation because it is adapted for the temperature range of planktonic foraminifera. However, many studies looking at calcification

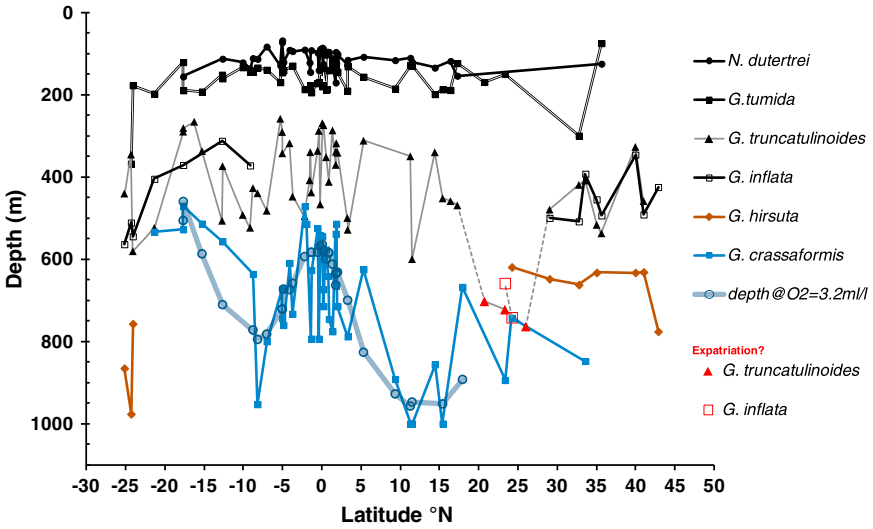

Figure 3. Calculated calcification depths versus latitude of the core top for each species. The depth of the 3.2 ml/l oxygen level is plotted with the blue thick line. The North subtropical gyre data of *G. inflata* and *G. truncatulinoides*, possibly affected by expatriation, are plotted in red.

Table 3. Correlation Coefficients and p Values for the Correlations Between Geochemical Measurements and Core Depths[a]

	G. crassaformis	*N. dutertrei*	*G. truncatulinoides*	*G. tumida*	*G. inflata*	*G. hirsuta*
			All data			
Mg/Ca versus depth	$r^2 = 0.12$, $p = 0.045$	$r^2 = 0.14$, $p = 0.02$	$r^2 = 0.17$, $p = 0.017$	$r^2 = 0.05$, $p = 0.15$	*$r^2 = 0.001$, $p = 0.94$*	*$r^2 < 0.001$, $p = 0.51$*
$\delta^{18}O$ versus depth	*$r^2 = 0.01$, $p = 0.44$*	*$r^2 = 0.13$, $p = 0.18$*	*$r^2 = 0.003$, $p = 0.71$*	*$r^2 = 0.001$, $p = 0.82$*	*$r^2 = 0.12$, $p = 0.44$*	*$r^2 = 0.04$, $p = 0.64$*
Mg/Ca versus T_{iso}	$r^2 = 0.43$, $p < 10^{-4}$	$r^2 = 0.42$, $p < 10^{-5}$	$r^2 = 0.59$, $p < 10^{-6}$	$r^2 = 0.60$, $p < 10^{-7}$	$r^2 = 0.71$, $p = 0.017$	$r^2 = 0.51$, $p = 0.07$
			Dissolution-free cores only			
Dissolution start at	4.4 km	4.0 km	4.0 km	4.4 km		
Mg/Ca versus depth	$r^2 = 0.23$, $p = 0.005$	*$r^2 = 0.09$, $p = 0.10$*	*$r^2 = 0.06$, $p = 0.19$*	*$r^2 = 0.015$, $p = 0.46$*		
$\delta^{18}O$ versus depth	*$r^2 = 0.04$, $p = 0.19$*	*$r^2 = 0.02$, $p = 0.37$*	*$r^2 = 0.004$, $p = 0.70$*	*$r^2 = 0.009$, $p = 0.51$*		
Mg/Ca versus T_{iso}	$r^2 = 0.42$, $p < 10^{-4}$	$r^2 = 0.50$, $p < 10^{-5}$	$r^2 = 0.60$, $p < 10^{-5}$	$r^2 = 0.60$, $p < 10^{-7}$		

[a]Data in italics indicate insignificant correlation.

depths for deep-dwelling species used the *Shackleton* [1974] $\delta^{18}O$-temperature relationship. We therefore also computed the $\delta^{18}O_{calc}$ with this equation (equation (2)). The different $\delta^{18}O$-temperature equations have been discussed in detail in other studies [*Bemis et al*., 1998; *Regenberg et al*., 2009] without clear consensus reached on which equation is most appropriate.

$$\delta^{18}O_{calc} = 5\left(4.38 - \sqrt{(4.38)^2 - 0.4 \times (16.9 - temp)}\right) + \left(\delta^{18}O_{calc} - 0.27\right) \quad (2)$$

3.6. Isotopic Temperature Calculation and Mg/Ca Calibrations

[17] Once the calcification depth is known, the isotopic temperature of calcification (T_{iso}) is calculated using the following equation (3).

$$T_{iso} = 16.1 - 4.64\left(\delta^{18}O_{foram} - \left(\delta^{18}O_{sw} - 0.27\right)\right) + 0.09\left(\delta^{18}O_{foram} - \left(\delta^{18}O_{sw} - 0.27\right)\right)^2 \quad (3)$$

Where $\delta^{18}Osw$ is taken at the calcification depth. The potential influence of salinity on the Mg/Ca ratio cannot be estimated here [*Arbuszewski et al*., 2010] because below 200 m depth, temperature and salinity are highly correlated along our transect (Figure S2 in supporting information, $r^2 = 0.89$ at 200 m depth and increasing further down).

[18] Assuming a linear equation for T_{iso} (neglecting the square term in equation (3)), the error on T_{iso} can be propagated from the error on $\delta^{18}O_{foram}$ and $\delta^{18}Osw$. The error on $\delta^{18}O_{foram}$ is expressed as the mean standard deviation of the replicate for each species, while the error on $\delta^{18}Osw$ is taken as the difference between T_{iso} calculated using equation (3) and T_{iso} calculated for a fixed $\delta^{18}Osw$ value (Table 2).

4. Results

4.1. Calcification Depths

[19] Each species has a distinct $\delta^{18}O$ signature (Figure 2), from the relatively depleted values of *G. ruber* and *N. dutertrei* to the enriched values of *G. crassaformis* and *G. hirsuta*. These differences reflect their different mean calcification depths. The highly scattered data between 4°N and 5°S reflect the complex temperature and salinity fields associated with the zonal equatorial circulation and indicate coherent zonal water column structure consistent with this circulation. For example, *N. dutertrei* reproduces very well the large amplitude changes seen in the temperature field at 100 m depth along the transect (Figure S1 in supporting information).

[20] Using the paleotemperature equation (equation (1)) [*Kim and O'Neil*, 1997] and comparing $\delta^{18}O_{calc}$ with $\delta^{18}O_{foram}$, we find an average calcification depth of 115 m for *N. dutertrei* (standard deviation (SD) is 22 m, standard error (SE) is 3.5 m); 160 m for *G. tumida* (SD 46 m, SE 6 m); 420 m for *G. truncatulinoides* (SD 115 m, SE 15 m); 475 m for *G. inflata* (SD 112 m, SE 27 m); 720 m for *G. hirsuta* (SD 120 m, SE 38 m); and 700 m for *G. crassaformis* (SD 152 m, SE 23 m) (Figure 3). For some species, the mean calcification depth masks large regional variation that will be discussed further. Equation (2) [*Shackleton*, 1974] yields shallower calcification depths: 100 m for *N. dutertrei*, 145 m for *G. tumida*, 300 m for *G. truncatulinoides*, 330 m for *G. inflata*, and 600 m for both *G. hirsuta* and *G. crassaformis*.

4.2. Mg/Ca-T_{iso} Calibrations

[21] Dissolution taking place in the deep ocean where carbonate ion approaches undersaturation affects shell Mg/Ca ratios. We examined the influence of dissolution on our

Table 4. Mg/Ca-T_{iso} Calibrations Using the Entire Data Set; the 95% Confidence Intervals Are Given for Each Coefficient[a]

	Mg/Ca = a exp(b T)				Error Calibration
	R^2	p	a	b	
N. dutertrei	0.42	2.2E−05	0.487 ± 0.015	0.074 ± 0.009	1.95
G. tumida	0.60	1.2E−08	0.392 ± 0.009	0.101 ± 0.010	1.22
G. truncatulinoides (d.)	0.59	2.1E−07	0.938 ± 0.030	0.066 ± 0.007	1.22
G. inflata South Atlantic	0.71	0.017	0.585 ± 0.050	0.133 ± 0.032	0.89
G. hirsuta (d.) North Atlantic	0.51	0.072	0.200 ± 0.076	0.184 ± 0.057	0.79
G. crassaformis (*s*.)	0.43	3.1E−05	0.658 ± 0.006	0.122 ± 0.016	0.82

[a]For the calibrations developed without the deepest samples, see equations in Figure 4.

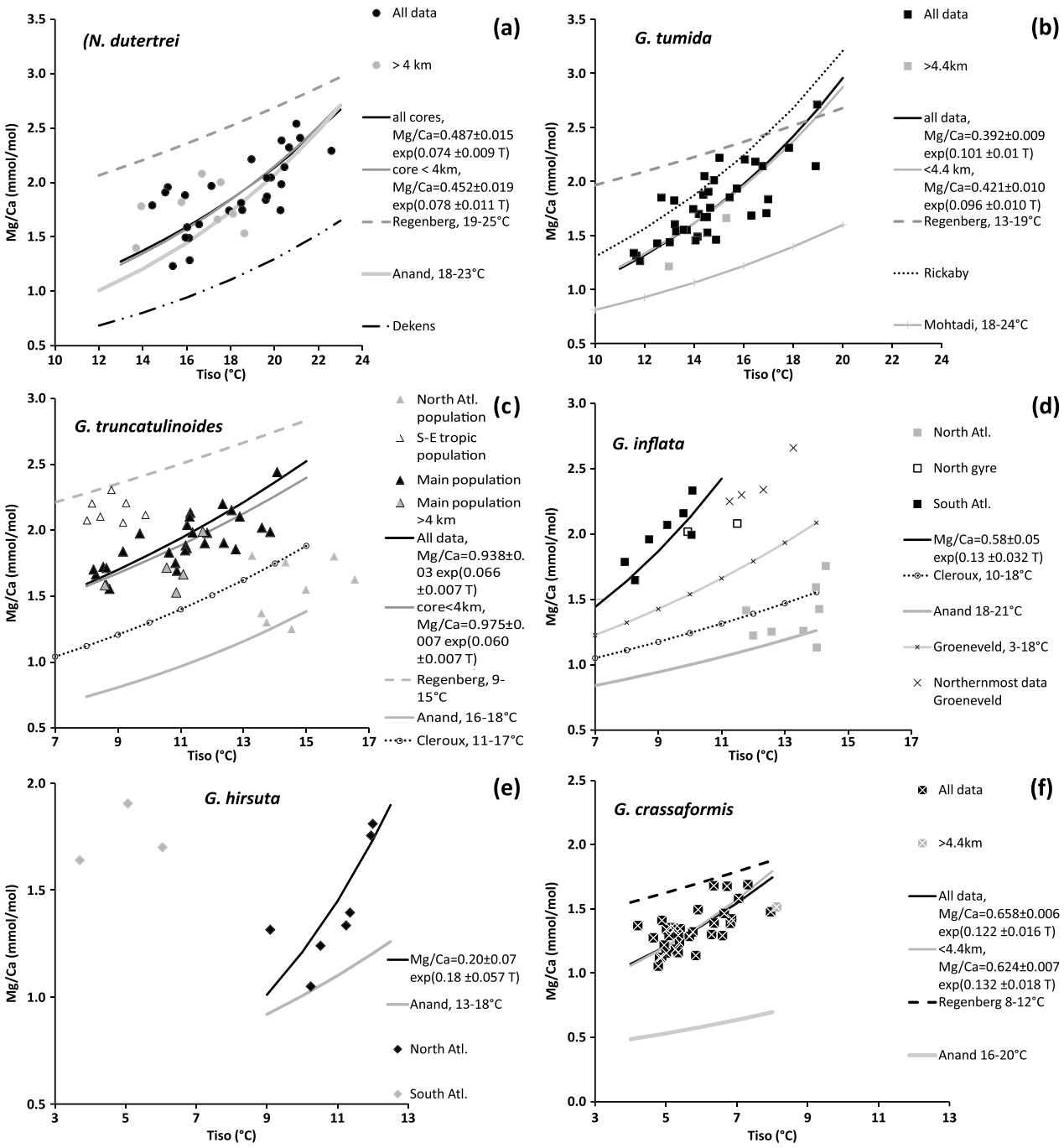

Figure 4. Mg/Ca-temperature relationships and comparison with previous calibrations for (a) *N. dutertrei*, (b) *G. tumida*, (c) *G. truncatulinoides*, (d) *G. inflata*, (e) *G. hirsuta*, and (f) *G. crassaformis*. Calibrations using the entire data sets are plotted in black; calibrations without the deepest samples (grey symbols) are plotted in grey. References are *Anand et al.* [2003], *Cléroux et al.* [2008], *Dekens et al.* [2002], *Groeneveld and Chiessi* [2011], *Haarmann et al.* [2011], *Regenberg et al.* [2009], and *Rickaby and Elderfield* [2005]; for aesthetic purpose only the first name of each study is written on the figure. For graphic comparison, previous calibrations are plotted over the temperature range relevant for the current study, but the ranges covered by previous works are indicated. For *N. dutertrei*, the *Dekens et al.* [2002] equation is plotted for depth = 3.7 km (mean value of each data set from this study).

results using the relationship between water depth of the samples or bottom ΔCO_3^{2-} and the Mg/Ca ratio (Figure S5 in supporting information and Table 3). Bottom water ΔCO_3^{2-} and water depth are highly correlated along this transect ($r^2 = 0.80$) and therefore yield very similar results for our study. *G. inflata* and *G. hirsuta* do not show any correlation between core depth and Mg/Ca or between ΔCO_3^{2-} and Mg/Ca. The trends observed for the other species are only statically significant when using core depth as opposed to bottom ΔCO_3^{2-}. Depth is a more

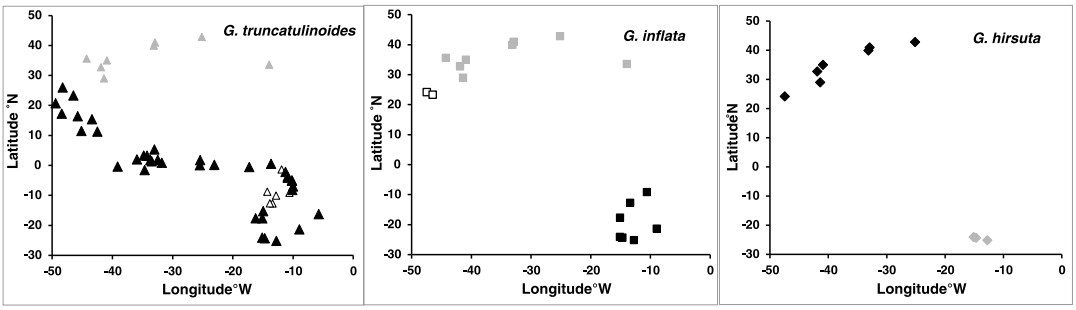

Figure 5. Locations of the various populations of *G. inflata*, *G. truncatulinoides*, and *G. hirsuta* as identified from the Mg/Ca-temperature relationships. Symbols are the same as in Figure 4.

straightforward parameter with no error and easy to use in paleo-studies; we decided to use this parameter over bottom ΔCO_3^{2-}. For *N. dutertrei*, *G. tumida*, *G. truncatulinoides*, and *G. crassaformis*, we determined the depths above which the correlation between depth and Mg/Ca is no longer significant, and we developed calibrations using both the full data set and excluding the deepest samples (Table 4).

[22] Several subpopulations along our transect with very different temperature-Mg/Ca relationships can be identified for *G. truncatulinoides*, *G. inflata*, and *G. hirsuta* (Figure 4). A northern and a southern population can be easily distinguished for both *G. hirsuta* and *G. inflata*. For *G. inflata*, two data points in the North Atlantic gyre at 24.2°N and 23.3°N plot with the data from the South Atlantic. These two data were not included in the calculation of the calibration. The Mg/Ca data for *G. truncatulinoides* suggest three distinct populations: one in the North Atlantic (north of 29°N), one in the southeastern tropical upwelling region, and the third and largest one spanning much of the remainder of our transect, from 26°N to 25°S. Our calibration is based on the most abundant data set, i.e., it excludes the North Atlantic and upwelling populations. The spatial distributions of these subpopulations are plotted in Figure 5, and the calibrations are summarized in Table 4. Using each species-specific calibration, we calculated $T_{Mg/Ca}$ from the measured Mg/Ca data, then the difference between $T_{Mg/Ca}$ and T_{iso}, and an estimate of the calibration error which was calculated as the standard deviation of $T_{Mg/Ca}$ minus T_{iso} (Table 4) [*Anand et al.*, 2003].

Table 5. Reported Foraminiferal "Vital Effects" From the Literature

	Disequilibrium (‰)	Size Fraction (μm)	Reference[a]
N. dutertrei	0.0 to −0.53	>350	1
	−0.2	NA	2
	0.61 to +0.05	>500	3
	−0.2	NA	7
G. tumida	0.0	>200	1
	0.0	NA	2
G. truncatulinoides	−0.3 to +0.2	>250	1
	+0.2	NA	2
	−0.10 to +0.16	350–450	4
	1.1	150–250	5
	−0.11	280–440	6
	0	NA	7
G. inflata	−0.4 to +0.4	>200	1
	+0.01 to +0.25	350–450	4
	0.94	150–250	5
	−0.2	NA	7
G. crassaformis	+0.2 to 0.0	250 to 500	1
	+0.2	NA	2
G hirsuta	−0.5 to +0.2‰	>200	1
	0	NA	7

[a]References: 1, [*Niebler et al.*, 1999]; 2, [*Steph et al.*, 2009]; 3, [*Spero et al.*, 2003]; 4, [*Loncaric et al.*, 2006]; 5, [*Mortyn and Charles*, 2003]; 6, [*Wilke et al.*, 2009]; 7, [*Deuser and Ross*, 1989].

5. Discussion

5.1. Variability in the Equatorial Region

[23] In the equatorial region, the $\delta^{18}O$ values for all species display a large range >1.5‰. This variability is also apparent in the data from the World Ocean Circulation Experiment Upper Ocean Thermal database (http://www.ewoce.org/), which is a compilation of temperature profiles acquired by commercial, fishing, and research vessels within the upper kilometer of the water column (Figure S1 in supporting information). Our multispecies foraminifera $\delta^{18}O$ data from this array of Atlantic cores indicates that we should be able to reconstruct this variability (Figure 2).

5.2. Other Factors Affecting Foraminiferal $\delta^{18}O$

[24] Not all planktonic foraminifera calcify in equilibrium with seawater but instead can have an apparent offset (vital effect) between the measured $\delta^{18}O$ and the theoretical value ($\delta^{18}O_{calc}$). Recent intratest $\delta^{18}O$ measurements showed, for example, vital effects as large as 1‰ in the planktonic foraminifera species *Neogloborotalia pachyderma* [*Kozdon et al.*, 2009]. These species-specific offsets can originate from a number of biological processes (symbiont activity, ontogeny) [*Rohling and Cooke*, 1999]. This offset is particularly difficult to estimate for species with broad vertical habitat ranges and species for which no culture data are available [*Spero and Lea*, 1996]. Consequently, there is no consensus on possible oxygen isotopic disequilibrium values for the species considered here. Table 5 shows the large spread, frequently centered about a zero offset, of disequilibria estimated from previous works for the species used in this study. For this reason, and also because nonsymbiotic species (in our case *G. inflata*, *G. truncatulinoides*, *G. crassaformis*, and *G. hirsuta*) are believed to precipitate their shell calcite at or close to equilibrium [*Fairbanks et al.*, 1980], we assume no vital effect in this study. Support for this assumption comes from the plot of $\delta^{18}O$ measurements versus latitude (Figure 2). The isotopic data show progressively more enriched values for those

species that we know to dwell at or well below the thermocline [*Ravelo and Fairbanks*, 1992]. Also, each species has a distinct meridional gradient profile, suggesting that a simple vital effect offset is not responsible for the observed meridional interspecies variability.

[25] Culture experiments [*Spero et al*., 1997] have suggested that carbonate ion concentration may influence the foraminiferal $\delta^{18}O$ and $\delta^{13}C$. In field samples, this effect is difficult to assess because $[CO_3^{2-}]$ and temperature are correlated in the oceans [*Broecker and Peng*, 1982]. Along our transect, only at approximately 100 m depth is $[CO_3^{2-}]$ weakly correlated with temperature ($r^2 = 0.55$, $p = 0.00$). Therefore, our best opportunity to distinguish a $[CO_3^{2-}]$ effect should be using the *N. dutertrei* data since that species appears to calcify close to this level. Plotting *N. dutertrei* $\delta^{18}O$ versus $[CO_3^{2-}]$ calculated at 100 m does not show any significant correlation ($r^2 = 0.05$, $p = 0.134$). In particular, data in the equatorial region show no evidence of being influenced by the observed low $[CO_3^{2-}]$ in that region. If we still assume a carbonate ion effect, using the 0.002 [*Bijma et al*., 1998] or 0.005 [*Spero et al*., 1997] slopes for symbiotic and nonsymbiotic species, respectively, in the calculation of the $\delta^{18}O_{calc}$, then all the $[CO_3^{2-}]$-corrected $\delta^{18}O_{calc}$ are larger than the noncorrected $\delta^{18}O_{calc}$, and the calcification depths will appear deeper for all the species. For example, *N. dutertrei* would have an apparent calcification depth 25 m deeper and *G. crassaformis* 100 m deeper.

[26] Some plankton net studies have shown that deep-dwelling species tend to concentrate in the deep-chlorophyll maximum (DCM) [*Fairbanks and Wiebe*, 1980; *Wilke et al*., 2009]. Other studies suggest that the calcification depth of some planktonic foraminifera species may be sensitive to water density [*Simstich et al*., 2003], although *Matsumoto and Lynch-Stieglitz* [2003] showed that this is clearly not the case for *G. truncatulinoides*. To test the plausibility of these ideas, we compared the foraminiferal $\delta^{18}O$ with the $\delta^{18}O_{calc}$, calculated at the DCM depth and at fixed density levels for each core-top location. The depth and temperature of the DCM were extracted from the Atlantic Meridional Transect program leg 14 (http://www.amt-uk.org/), and then the $\delta^{18}O_{calc}$ was calculated according to equation (1). For isopycnal $\delta^{18}O_{calc}$, we used the Ocean Data View (ODV) program and the WOA database to extract the temperature on specific density levels at each core site and calculated $\delta^{18}O_{calc}$ with equation (1). We observe no correlation between the foraminiferal $\delta^{18}O$ and the δ^{18}Ocalc at DCM depth or δ^{18}Ocalc for fixed density levels (Figure S3 in supporting information), indicating no apparent correlation between calcification depth and water density or the DCM.

5.3. Dissolution Effect

[27] The effect of dissolution on the shell $\delta^{18}O$ composition is well known but rather subtle outside very corrosive water [*Erez*, 1979; *Johnstone et al*., 2011; *Savin and Douglas*, 1973]. In our data $\delta^{18}O$ is not correlated with depth (Table 3). Regarding the Mg/Ca ratios, early studies observed a decrease as dissolution or water depth (bottom ΔCO_3^{2-}) increases (decreases) [*Brown and Elderfield*, 1996; *Lohmann*, 1995; *Rosenthal et al*., 2000]. Some studies indicate that dissolution effects on planktonic foraminiferal Mg/Ca ratios can occur well above the calcite saturation horizon [Brown and Elderfield, 1996; *Johnstone et al*., 2011; *Regenberg et al*., 2006]. Dissolution affects both proxies to make the sample appear colder, with the amplitude of the effect being species-specific [*Berger*, 1970a; *Johnstone et al*., 2010; *Mekik et al*., 2007].

[28] Hence, dissolution-corrected Mg/Ca calibrations have flourished. It is, however, not clear how well these corrections perform. Using the depth-corrected Mg/Ca calibration for the Atlantic Ocean of *Dekens et al*. [2002], *Hönisch et al*. [2013] cleverly demonstrated that the correction is too large for cores between 2.8 and 4.4 km and too small for cores below 4.4 km. In addition, using bottom ΔCO_3^{2-} to correct for dissolution appears difficult to apply back in time.

[29] In our data, the trends between depth and Mg/Ca for *N. dutertrei*, *G. truncatulinoides*, and *G. tumida* become statistically insignificant when selecting the cores above 4 or 4.4 km (see Table 3). The Mg/Ca of *G. inflata* and *G. hirsuta* shows no sign of dissolution. This is in agreement with published data for the Atlantic Ocean where a careful examination shows a significant decrease in Mg/Ca only in the deepest cores, below 4.4 or 4.5 km [*Dekens et al*., 2002; *Rosenthal and Boyle*, 1993].

[30] Taking the entire data set for *G. crassaformis* (including a sample at 4.5 km depth), Mg/Ca shows only a weak correlation with depth ($r^2 = 0.12$, $p = 0.045$). However, this relation becomes stronger when ignoring this deepest sample ($r^2 = 0.23$, $p = 0.05$), and most importantly we then also observe a weak correlation between $\delta^{18}O$ and depth ($r^2 = 0.12$, $p = 0.025$). These relationships are only marginally significant statistically, but as they are both consistent with a modest dissolution effect (Mg/Ca decreases, $\delta^{18}O$ increases as depth increases), we examine this issue more closely. If dissolution had a strong influence on the samples, the $\delta^{13}C$ [*Lohmann*, 1995; *Rosenthal et al*., 2000] and the Sr/Ca [*Brown and Elderfield*, 1996] should both decrease with depth. $\delta^{13}C$ and Sr/Ca of *G. crassaformis* show no statistical correlation with depth (Table 3), and we conclude that dissolution is not responsible for the relationship between depth and $\delta^{18}O$ and Mg/Ca.

[31] In conclusion, our data set is not strongly affected by dissolution, but we still developed calibrations rejecting the deepest samples. However, the link between dissolution (as depth or bottom ΔCO_3^{2-}) should always be carefully assessed when applying back in time.

5.4. Mg/Ca Ratios and Previous Mg/Ca-Temperature Relationships (Figure 4)

[32] We consider two separate calibrations for four of the six species analyzed. One calibration uses all data, and one uses a subset of the full data set that removed the deepest and potentially most dissolution-affected samples as discussed above (Figure 4; see Table 3 for the species-specific depth threshold). The two calibrations are only distinguishable for one species, *G. truncatulinoides*, with a 0.8°C difference expressed for Mg/Ca = 2.4 mmol/mol. Most previous calibrations for deep-dwellers have been established using the cleaning procedure of *Barker et al*. [2003], as opposed to the reductive-oxidative protocol used here. Exceptions are for the *G. tumida* equation presented by *Rickaby and Elderfield* [2005] and the two equations for *N. dutertrei* from *Dekens et al*. [2002]. We typically found a greater slope but a lower pre-exponential constant for our calibrations compared with the work of *Regenberg et al*. [2009]. The lower pre-exponential constant may be partly explained by differences in the cleaning protocols [*Barker et al*., 2003] and partly by the more restrictive size fraction (355–400 μm) used by *Regenberg et al*. [2009]. Some of their

specimens may have been devoid of the low-Mg calcite crust covering the shells [*Sadekov et al*., 2005]. It should also be noted that their data sets cover only the warmest part of our calibration for *N. dutertrei*. For *G. crassaformis*, the two calibrations would probably agree if the calibrations had overlapped at warmer temperature. For *G. tumida*, the coldest part of the *Regenberg et al*. [2009] calibration for this species displays large Mg/Ca scatter (> 1 mmol/mol at 14°C). Considering this spread, their data would also agree with our calculated slope. We also note a good agreement between our data and a Pacific equatorial calibration for *G. tumida* [*Rickaby and Elderfield*, 2005]. Surprisingly, our calibration for *N. dutertrei* is almost identical to the *Anand et al*. [2003] calibration, developed on sediment trap material in the Sargasso Sea. On the other end of the spectrum, our calibration for *G. crassaformis* shows much higher Mg/Ca ratios than those of *Anand et al*. [2003]. This discrepancy may originate from the different sample type (core top versus sediment trap) and also because these two data sets cover completely different temperature ranges (4–8°C for this work versus 16–20°C for Anand's calibration [*Martínez-Botí et al*., 2011]). Considering only the North Atlantic populations of *G. truncatulinoides* and *G. inflata*, the *Anand et al*. [2003] and *Cléroux et al*. [2008] calibrations match our data, which confirms the different Mg/Ca to temperature relationships for these North Atlantic populations.

[33] The calibration developed from South Atlantic core tops along the South American margin spanning 20°S–50°S for *G. inflata* [*Groeneveld and Chiessi*, 2011] does not fit with our calibration for this species. This is not surprising since *Groeneveld and Chiessi* [2011] used non-encrusted shells in contrast to the current study. However, the few samples from the *Groeneveld and Chiessi* [2011] study that overlap our study region have much higher Mg/Ca ratios and, as such, are in line with our data set for the South Atlantic (Figure 4d). Along with a small number of calibration points provided by *Anand et al*. [2003] for *G. hirsuta*, we provide the first calibration for this species.

[34] Finally, we measured much higher Mg/Ca ratios in *N. dutertrei* and in *G. tumida* than *Dekens et al*. [2002] and [*Mohtadi et al*., 2011], respectively. *Dekens et al*. [2002] used slightly smaller specimens (250–350 μm) but the same cleaning protocol, whereas *Mohtadi et al*. [2011] used larger specimens (355–500 μm) and the oxidative-only cleaning protocol. It is difficult to single out why these two studies present such low Mg/Ca ratios, but *Dekens et al*. [2002] samples come from both the Atlantic and the Pacific Ocean and *Mohtadi et al*. [2011] samples come from the Indonesian Margin. *Mohtadi et al*. [2011] studied several species, and in general their calibrations fit well with previous works except for one species, *G. tumida*. According to the authors, this species in the Indonesian Seas may have a specific habitat or ecology. We can only speculate that this is also the case for *N. dutertrei* in the Pacific Ocean in the case of *Dekens et al*. [2002] calibration.

5.5. *Neogloboquidrina dutertrei* and *Globorotalia tumida*

[35] From both $\delta^{18}O$ and Mg/Ca data, these two species seem to have homogeneous populations across our study area, with a single Mg/Ca-T relationship for each species and remarkably narrow calcification depth ranges of 90–135 and 115–205 m, respectively, for *N. dutertrei* and *G. tumida*. This is in agreement with other core-top investigations in the tropical Atlantic [*Farmer et al*., 2007; *Regenberg et al*., 2009; *Steph et al*., 2009] and with isotopic measurements from sediment trap material [*Deuser and Ross*, 1989; *Mohtadi et al*., 2011]. It does not appear that the depth habitats of these species are governed by temperature, as the reconstructed T_{iso} values for *G. tumida* changes by 11°C for example. One would expect a much smaller temperature range if *G. tumida* was seeking a certain temperature in the water column to grow.

[36] The carbon stable isotopic ($\delta^{13}C$) results (Figure S4 in supporting information) support observations of living specimens [*Ortiz et al*., 1995] in indicating that *N. dutertrei* and *G. tumida* have algal symbionts. Symbionts may have light requirements in a specific range, which may then restrict the calcification/habitat depths of the host (H. Spero, personal communication). As an illustration of this, we applied the relationship between $\delta^{13}C$ and irradiance deduced from an *Orbulina universa* laboratory experiment [*Spero and Wiliams*, 1989] and the relationship between depth and irradiance (Beer-Lambert law) to our *N. dutertrei* and *G. tumida* data, $I_z = I_0 \times \exp(-kZ)$, where I_z is the irradiance at depth z; I_0 is the irradiance at the surface ($I_0 = 2300\ \mu E\ m^{-2}\ s^{-1}$); and k is the attenuation coefficient ($k = 0.04$ in open-ocean condition); $\delta^{13}C = 1.50 \times I^{0.106}$ [*Spero and Wiliams*, 1989].

[37] In our samples, *N. dutertrei* and *G. tumida* have a $\delta^{13}C$ of about 2‰ (Figure S4 in supporting information). If we assume that both species have a similar relationship between $\delta^{13}C$ and irradiance as *O. universa*, we can calculate at what depth in the open ocean this irradiance level is reached. We found $I = 15.8\ \mu E\ m^{-2}\ s^{-1}$ and $z = 125$ m. This depth is similar to the calcification depth deduced from the $\delta^{18}O$ measurements. The strict irradiance requirements of some symbiotic algae may offer a valid hypothesis for why we observe such a narrow depth habitat for these hosts.

5.6. *Globorotalia inflata*

[38] *G. inflata* is a transitional species and is therefore abundant only at both latitudinal extremes of our transect. The Mg/Ca data clearly separate a northern and a southern population that have similar calcification depths (450 ± 60 and 440 ± 100 m, respectively). In the North Atlantic, two data points from 23°N to 24°N contradict these observations; they have much deeper estimated calcification depths (740 and 660 m), and their Mg/Ca-temperature relationship fits more closely with the overall data from the South Atlantic.

[39] It is tempting to attribute the two distinct Mg/Ca-temperature relationships for the northern and southern data as potentially reflecting separate genotypes. So far, two cryptic species distributed on each side of the Antarctic Subpolar Front have been identified for *G. inflata* [*Morard et al*., 2011], but the subtropical regions have been poorly investigated. Using laser-ablation Mg/Ca measurement on sediment trap material [*Hathorne et al*., 2009], two types of *G. inflata* were found with mean Mg/Ca ratios about 1 mmol/mol apart, although all the tests were collected over a two-week period. The author concluded this resulted from a large influence of short-time-scale (daily) conditions on shell geochemistry and morphology.

[40] The two data points at 23°N–24°N may suggest a third genetic population. However, these specimens lie far from the typical geographic distribution zone of *G. inflata* [*Bé*, 1977]. It is therefore possible that they reflect a stressed population or expatriated specimens.

[41] *G. inflata* is a widely used deep-dwelling planktonic foraminifera species for paleoceanographic reconstructions. The existence of several genetic species with different Mg/Ca-temperature relationships calls for caution when using this species for paleoclimate study.

5.7. *Globorotalia truncatulinoides*

[42] Similar to *G. inflata*, we can identify three distinct *G. truncatulinoides* populations from the Mg/Ca data, although the calcification depths, determined from foraminiferal $\delta^{18}O$, are generally similar. Like *G. inflata*, three samples in the northern subtropical gyre show much deeper calcification depth. The three samples at 20°N, 23°N, and 26°N have a mean calcification depth of 730 ± 30 m, whereas the calculation for the rest of the samples yields 400 ± 90 m. The occurrence of these three populations is not surprising with respect to the different genetic species grouped together under the *G. truncatulinoides* morphospecies [*de Vargas et al*., 2001; *Quillévéré et al*., 2013]. These studies showed that the different cryptic species can have different ecological preferences in terms of water dynamics, nutrient availability, and possible water depth habitat preference [*de Vargas et al*., 2001]. Four dextral genotypes have been identified in the Atlantic Ocean, and it is possible that the three populations defined here from Mg/Ca ratios correspond to these genetically distinct species (Figure 5).

[43] Previous isotopic studies found *G. truncatulinoides* to be at equilibrium with conditions at various depths: at 200 m in the Sargasso Sea [*Deuser and Ross*, 1989], at 350 m in the Canary Islands region [*Wilke et al*., 2009], and between 270 and 370 m along a longitudinal transect in the equatorial Atlantic [*Steph et al*., 2009]. *Cléroux et al*. [2007] showed that *G. truncatulinoides* has a deeper mean calcification depth in the warm subtropical regions (between 200 and 400 m) than at temperate latitudes. Using a large data set in the Atlantic Ocean, *Legrande et al*. [2004] found the calcification depth best represented by a single calcification depth of 350 m or a two-depth calcification with 30% at the surface and 70% at 800 m. With these separate studies, it is hard to ascertain whether these discrepancies are related to various locations, size fractions, material types, or different $\delta^{18}O$-temperature equations used. Excluding the data from the northern subtropical gyre, we show that from 40°N to 25°S, *G. truncatulinoides* calcify around 400 ± 90 m but present a number of Mg/Ca-temperature calibrations depending on the region.

[44] The *G. inflata* and *G. truncatulinoides* results for the northern subtropical gyre (20°N–26°N) deserve further discussion. For both species, $\delta^{18}O$ data indicate a very deep calcification depth, whereas their Mg/Ca ratios are either in agreement (*G. truncatulinoides*) or disagreement (*G. inflata*) with the other data. We can discard dissolution as an explanation because other species do not show any specific pattern for these core tops, and dissolution would lower the Mg/Ca ratio, which would directly contradict our observations. Foraminifera, and particularly deep-dwelling species with a long life span [*Schiebel and Hemleben*, 2005], may be affected by expatriation, where shells are transported over long distances [*Berger*, 1970b]. These distinctive samples are located in the main circulation path of the northern STC [*Harper*, 2000]. We can hypothesize that *G. truncatulinoides* and *G. inflata* were transported within the thermocline from the subduction zone. Considering a subduction zone centered around 30°N–30°W [*Harper*, 2000], we recalculated the fit between foraminiferal data and atlas data. If foraminifera did grow around 30°N–30°W, then their calcification depth would be in better agreement with the rest of the transect results (i.e., around 550 m depth). The Mg/Ca-temperature data for *G. inflata* would converge on the data from the northern population (i.e., warmer temperature), although in this instance the Mg/Ca-temperature data for *G. truncatulinoides* would no longer fit with the calibration for this species. We cannot be conclusive on the expatriation hypothesis from these rough calculations, but we still judge it likely. Other species living shallower or deeper in the water column are much less likely to be in the main STC path and would not be affected by this transport.

5.8. *Globorotalia hirsuta* and *Globorotalia crassaformis*

[45] Both isotope and trace element data for *G. hirsuta* indicate two distinct populations, the North Atlantic (South Atlantic) population calcifies around 660 m (860 m) and yields lower Mg/Ca ratios than the South Atlantic population. To our knowledge, this study is the first to report on this species, and presently no genetic studies are available.

[46] *G. crassaformis* forms one single population with an average calcification depth of 700 m. The habitat depth of these two species has been poorly documented. Using the *Kim and O'Neil* [1997] equation, isotope data in the tropical Atlantic core-tops indicate a calcification depth near 600 m for *G. crassaformis* [*Steph et al*., 2009]. From sediment trap analysis in the Sargasso Sea, *Deuser and Ross* [1989] concluded that *G. hirsuta* calcify near 600 m.

[47] The calcification depth of *G. crassaformis* is symmetric about the equator (Figure 3), with shallower depth in the equatorial region, greater depths in the subtropical regions, and then a shoaling toward higher latitudes. This structure cannot be fortuitous, and we tested our data against various oceanographic parameters to explain the results. Of all the parameters tested (temperature, salinity, density, nutrient concentrations), only dissolved oxygen levels along our transect show a pattern similar to *G. crassaformis* calcification depth. We find a good match between the calcification depth of *G. crassaformis* and the depth of the 3.2 ml/l oxygen level (Figures 1 and 3). This is consistent with abundant *G. crassaformis* found at the minimum oxygen level in the water column in the eastern equatorial Atlantic [*Kemle von Mücke and Oberhänsli*, 1999]. The observed deep habitat depth may seem odd, but benthic foraminifera, for example, are abundant in low oxygen environments, probably because the predation pressure is much lower [*Bernhard and Sen Gupta*, 2000]. Other organisms have also been shown to thrive right below the oxygen minimum zone and consume aggregates that originate from bacterial activity in the oxygen minimum zones underlying the high productive areas [*Gowing and Wishner*, 1998].

6. Conclusions

[48] For the first time the calcification depths and Mg/Ca-temperature relationships of six deep-dwelling foraminifera species are determined over an Atlantic Ocean basin transect spanning more than 60° in latitude. We found that *N. dutertrei* and *G. tumida* maintain the same calcification depth throughout the wide range of oceanographic conditions, respectively 115 ± 25 and 160 ± 45 m, and we developed new Mg/Ca-temperature calibrations for these species. We propose that the

calcification depths of *N. dutertrei* and *G. tumida* are constrained by the light requirements of their symbionts. For three species (*G. inflata*, *G. truncatulinoides*, and *G. hirsuta*) the change in Mg/Ca-temperature relationship with sample location points to distinct populations or genotypes. For *G. hirsuta*, the North Atlantic and South Atlantic populations also have different calcification depth, whereas the subpopulations of *G. inflata* and *G. truncatulinoides* have similar calcification depths. In the northern subtropical gyre, we calculated a very deep calcification depth for *G. inflata* and *G. truncatulinoides* outside the range of depths calculated for the rest of the transect. One hypothesis for this result is expatriation of specimens via the subtropical cell.

[49] Finally, we suggest that *G. crassaformis* calcifies close to the oxygen minimum zone in the water column. We developed a Mg/Ca-temperature calibration for this species which further paves the way for deep-thermocline, O_2 minimum-level reconstructions.

[50] **Acknowledgments.** We thank Rusty Lotti and Nichole Anest, who provided access to samples from the Lamont Core Repository, and Stephen Howe (SUNY Albany) for the isotopic analysis. Great thanks go to G. Mortyn, M. Regenberg, and one anonymous reviewer; their comments greatly improved the manuscript. This research was supported in part by NSF awards OCE-0927247 and OCE-07-52649 (both to P. deMenocal), the Lamont Climate Center, and the Center for Climate and Life. Data presented in this study are available at the PANGAEA data center.

References

Anand, P., H. Elderfield, and M. H. Conte (2003), Calibration of Mg/Ca thermometry in planktonic foraminiferal from a sediment trap series, *Paleoceanography*, *18*(2), 1050, doi:10.1029/2002PA000846.

Antonov, J. I., D. Seidov, T. P. Boyer, R. A. Locarnini, A. V. Mishonov, H. E. Garcia, O. K. Baranova, M. M. Zweng, and D. R. Johnson (2010), *World Ocean Atlas 2009,* Volume 2*: Salinity*, 184 pp., U.S. Government Printing Office, Washington, D.C.

Arbuszewski, J. J., P. B. deMenocal, A. Kaplan, and C. E. Farmer (2010), On the fidelity of shell-derived δ18Oseawater estimates, *Earth Planet. Sci. Lett.*, *300*(3-4), 185–196, doi:10.1016/j.epsl.2010.10.035.

Barker, S., M. Greaves, and H. Elderfield (2003), A study of cleaning procedures used for foraminiferal Mg/Ca paleothermometry, *Geochem. Geophys. Geosyst.*,, *4*(9), 8407, doi:10.1029/2003gc000559.

Barker, S., I. Cacho, H. Benway, and K. Tachikawa (2005), Planktonic foraminiferal Mg/Ca as a proxy for past oceanic temperatures: A methodological overview and data compilation for the Last Glacial Maximum, *Quat. Sci. Rev.*, *24*(7–9), 821–834, doi:10.1016/j.quascirev.2004.07.016.

Bé, A. W. H. (1977), An ecological, zoogeographic and taxonomic review of recent planktonic foraminifera, in *Oceanic Micropaleontology*, edited by A. T. S. E. Ramsay, pp. 1–100, Academic press, London.

Bé, A. W. H., and D. S. Tolderlund (1971), Distribution and ecology of living foraminifera in surface waters of the Atlantic and Indian ocean, in *The Micropaleontology of Oceans*, edited by B. M. Funnel and W. R. Riedel, pp. 105–149, Cambridge Univ. Press, Cambridge, UK.

Bé, A. W. H., C. Hemleben, O. R. Anderson, M. Spindler, J. Hacunda, and S. Tuntivate-Choy (1977), Laboratory and field observation of living planktonic foraminifera, *Micropaleontology*, *23*(2), 155–179.

Bemis, B. E., H. J. Spero, J. Bijma, and D. W. Lea (1998), Reevaluation of the oxygen isotopic composition of planktonic foraminifera: Experimental results and revised paleotemperature equations, *Paleoceanography*, *13*(2), 150–160, doi:10.1029/98pa00070.

Berger, W. H. (1970a), Planktonic foraminifera: Selective solution and the lysocline, *Mar. Geol.*, *8*(2), 111–138, doi:10.1016/0025-3227(70)90001-0.

Berger, W. H. (1970b), Planktonic foraminifera: Differential production and expatriation off Baja, California, *Limnol. Oceanogr.*, *15*(2), 183–204.

Berger, W. H., J. S. Killingley, C. V. Metzler, and E. Vincent (1985), Two-step deglaciation: ^{14}C-dated high-resolution δ18O records from the tropical Atlantic Ocean, *Quat. Res.*, *23*(2), 258–271, doi:10.1016/0033-5894(85)90032-8.

Bernhard, J. M., and B. K. Sen Gupta (2000), Foraminifera of oxygen-depleted environment, in *Modern Foraminifera*, edited by B. K. Sen Gupta, pp. 201–216, Kluwer Academic Press, Dordrecht.

Bijma, J., H. J. Spero, and D. W. Lea (1998), Oceanic carbonate chemistry and foraminiferal isotopes: New laboratory results, in *Sixth International Conference on Paleoceanography*, Lisbon

Boccaletti, G., R. Ferrari, A. Adcroft, D. Ferreira, and J. Marshall (2005), The vertical structure of ocean heat transport, *Geophys. Res. Lett.*, *32*, L10603, doi:10.1029/2005gl022474.

Boyle, E. A., and L. D. Keigwin (1985), Comparison of Atlantic and Pacific paleochemical records for the last 215,000 years: Changes in deep ocean circulation and chemical inventories, *Earth Planet. Sci. Lett.*, *76*, 135–150.

Broecker, W. S., and T. H. Peng (1982), *Tracers in the Sea*, 690 pp., Lamont-Doherty Geological Observatory, Columbia University, New York.

Broecker, W. S., Y. Lao, M. Klas, E. Clark, G. Bonani, S. Ivy, and C. Chen (1993), A search for an Early Holocene $CaCO_3$ preservation event, *Paleoceanography*, *8*(3), 333–339, doi:10.1029/93pa00423.

Broecker, W., E. Clark, I. Hajdas, and G. Bonani (2004), Glacial ventilation rates for the deep Pacific Ocean, *Paleoceanography*, *19*, PA2002, doi:10.1029/2003PA000974.

Brown, S. J., and H. Elderfield (1996), Variations in Mg/Ca and Sr/Ca ratios of planktonic foraminifera caused by postdepositional dissolution: Evidence of shallow Mg-dependent dissolution, *Paleoceanography*, *11*(5), 543–551, doi:10.1029/96pa01491.

Cléroux, C., E. Cortijo, J. C. Duplessy, and R. Zahn (2007), Deep-dwelling foraminifera as thermocline temperature recorders, *Geochem. Geophys. Geosyst.*, *8*(4), doi:10.1029/2006GC001474.

Cléroux, C., E. Cortijo, P. Anand, L. Labeyrie, F. Bassinot, N. Caillon, and J.-C. Duplessy (2008), Mg/Ca and Sr/Ca ratios in planktonic foraminifera: Proxies for upper water column temperature reconstruction, *Paleoceanography*, *23*, PA3214, doi:10.1029/2007pa001505.

Cléroux, C., P. deMenocal, and T. Guilderson (2011), Deglacial radiocarbon history of tropical Atlantic thermocline waters: Absence of CO2 reservoir purging signal, *Quat. Sci. Rev.*, *30*(15–16), 1875–1882, doi:10.1016/j.quascirev.2011.04.015.

Darling, K. F., M. Kucera, D. Kroon, and C. M. Wade (2006), A resolution for the coiling direction paradox in *Neogloboquadrina pachyderma*, *Paleoceanography*, *21*, PA2011, doi:10.1029/2005PA001189.

Dekens, P. S., D. W. Lea, D. K. Pak, and H. J. Spero (2002), Core top calibration of Mg/Ca in the tropical foraminifera: Refining paleotemperature estimation, *Geochem. Geophys. Geosyst.*, *3*(4), 1022, doi:10.1029/2001GC000200.

Deuser, W. G., and E. H. Ross (1989), Seasonally abundant planktonic foraminifera of the Sargasso Sea; succession, deep-water fluxes, isotopic compositions, and paleoceanographic implications, *J. Foraminiferal Res.*, *19*(4), 268–293, doi:10.2113/gsjfr.19.4.268.

de Vargas, C., S. Renaud, H. Hilbrecht, and J. Pawlowski (2001), Pleistocene adaptive radiation in *Globorotalia truncatulinoides* : Genetic, morphologic, and environmental evidence, *Paleobiology*, *27*(1), 104–125.

Epstein, S., R. Buchbaum, H. A. Lowenstam, and H. C. Urey (1953), Revised carbonate-water isotopic temperature scale, *Bull. Geol. Soc. Am.*, *64*, 1315–1326.

Erez, J. (1979), Modification of the oxygen-isotope record in deep-sea cores by Pleistocene dissolution cycles, *Nature*, *281*, 535–538.

Ericson, D. B., and G. Wollin (1968), Pleistocene climates and chronology in deep-sea sediments, *Science*, *162*(3859), 1227–1234.

Ericson, D. B., G. Wollin, and J. Wollin (1954), Coiling direction of *Globorotallia truncatulinoides* in deep-sea cores, *Deep Sea Res.*, *2*, 152–158.

Fairbanks, R. G., and P. H. Wiebe (1980), Foraminifera and chlorophyll maximum: Vertical distribution, seasonal succession, and paleoceanographic significance, *Science*, *209*(4464), 1524–1526.

Fairbanks, R. G., P. H. Wiebe, and A. W. H. Bé (1980), Vertical distribution and isotopic composition of living planktonic foraminifera in the western North Atlantic, *Science*, *207*(4426), 61–63.

Farmer, E. C., A. Kaplan, P. B. de Menocal, and J. Lynch-Stieglitz (2007), Corroborating ecological depth preferences of planktonic foraminifera in the tropical Atlantic with the stable oxygen isotope ratios of core top specimens, *Paleoceanography*, *22*, PA3205, doi:10.1029/2006pa001361.

Fratantoni, D. M., W. E. Johns, T. L. Townsend, and H. E. Hurlburt (2000), Low-latitude circulation and mass transport pathways in a model of the tropical Atlantic Ocean, *J. Phys. Oceanogr.*, *30*(8), 1944–1966, doi:10.1175/1520-0485(2000)030<1944:llcamt>2.0.co;2.

Ganssen, G., and D. Kroon (2000), The isotopic signature of planktonic foraminifera from NE Atlantic surface sediments: Implications for the reconstruction of past oceanic conditions, *J. Geol. Soc. London*, *157*, 693–699, doi:10.1144/jgs.157.3.693May 2000.

Garcia, H. E., R. A. Locarnini, T. P. Boyer, J. I. Antonov, O. K. Baranova, M. M. Zweng, and D. R. Johnson (2010a), *World Ocean Atlas 2009, Volume 3: Dissolved Oxygen, Apparent Oxygen Utilization, and Oxygen Saturation*, U.S. Government Printing Office, Washington, D.C., pp. 344 .

Garcia, H. E., R. A. Locarnini, T. P. Boyer, J. I. Antonov, M. M. Zweng, O. K. Baranova, and D. R. Johnson (2010b), *World Ocean Atlas 2009, Volume 4: Nutrients (Phosphate, Nitrate, Silicate)*, U.S. Government Printing Office, Washington, D.C.

Gowing, M. M., and K. F. Wishner (1998), Feeding ecology of the copepod *Lucicutia aff. L. grandis* near the lower interface of the Arabian Sea oxygen

minimum zone, *Deep Sea Res., Part II*, *45*, 2433–2459, doi:10.1016/S0967-0645(98)00077-0.

Greaves, M., et al. (2008), Interlaboratory comparison study of calibration standards for foraminiferal Mg/Ca thermometry, *Geochem. Geophys. Geosyst.*, *9*, Q08010, doi:10.1029/2008gc001974.

Groeneveld, J., and C. M. Chiessi (2011), Mg/Ca of Globorotalia inflata as a recorder of permanent thermocline temperatures in the South Atlantic, *Paleoceanography*, *26*, PA2203, doi:10.1029/2010pa001940.

Gu, D., and S. G. H. Philander (1997), Interdecadal climate fluctuations that depend on exchanges between the tropics and the extratropics, *Science*, *275*(5301), 805–807, doi:10.1126/science.275.5301.805.

Haarmann, T., E. C. Hathorne, M. Mohtadi, J. Groeneveld, M. Kölling, and T. Bickert (2011), Mg/Ca ratios of single planktonic foraminifer shells and the potential to reconstruct the thermal seasonality of the water column, *Paleoceanography*, *26*, PA3218, doi:10.1029/2010pa002091.

Harper, S. (2000), Thermocline ventilation and pathways of tropical-subtropical water mass exchange, *Tellus*, *52A*, 330–345, doi:10.1034/j.1600-0870.2000.d01-7.x.

Hathorne, E. C., R. H. James, and R. S. Lampitt (2009), Environmental versus biomineralization controls on the intratest variation in the trace element composition of the planktonic foraminifera *G. inflata* and *G. scitula*, *Paleoceanography*, *24*, PA4204, doi:10.1029/2009pa001742.

Hönisch, B., K. A. Allen, D. W. Lea, H. J. Spero, S. M. Eggins, J. Arbuszewski, P. de Menocal, Y. Rosenthal, A. D. Russell, and H. Elderfield (2013), The influence of salinity on Mg/Ca in planktic foraminifers—Evidence from cultures, core-top sediments and complementary $\delta^{18}O$, *Geochim. Cosmochim. Acta*, *121*(0), 196–213, doi:10.1016/j.gca.2013.07.028.

Hut, G. (1987), Consultants group meeting on stable isotope reference samples for geochemical and hydrological investigations, Vienna, Austria.

Johnstone, H. J. H., M. Schulz, S. Barker, and H. Elderfield (2010), Inside story: An X-ray computed tomography method for assessing dissolution in the tests of planktonic foraminifera, *Mar. Micropaleontol.*, *77*(1–2), 58–70, doi:10.1016/j.marmicro.2010.07.004.

Johnstone, H. J. H., J. Yu, H. Elderfield, and M. Schulz (2011), Improving temperature estimates derived from Mg/Ca of planktonic foraminifera using X-ray computed tomography-based dissolution index, XDX, *Paleoceanography*, *26*, PA1215, doi:10.1029/2009pa001902.

Kemle von Mücke, S., and H. Oberhänsli (1999), The distribution of living planktic foraminifera in relation to southeast Atlantic oceanography, in *Use of Proxies in Paleoceanography: Examples from South Atlantic*, edited by G. Fisher and G. Wefer, pp. 91–115, Springer, Berlin.

Kim, S. T., and J. R. O'Neil (1997), Equilibrium and non-equilibrium oxygen isotope effects in synthetic carbonates, *Geochim. Cosmochim. Acta*, *61*, 3461–3475, doi:10.1016/S0016-7037(97)00169-5.

Kozdon, R., T. Ushikubo, N. T. Kita, M. Spicuzza, and J. W. Valley (2009), Intratest oxygen isotope variability in the planktonic foraminifer *N. pachyderma*: Real vs. apparent vital effects by ion microprobe, *Chem. Geol.*, *258*, 327–337, doi:10.1016/j.chemgeo.2008.10.032.

LeGrande, A. N., J. Lynch-Stieglitz, and E. C. Farmer (2004), Oxygen isotopic composition of *Globorotalia truncatulinoides* as a proxy for intermediate depth density, *Paleoceanography*, *19*(PA4025), doi:10.1029/2004PA001045.

LeGrande, A. N., and G. A. Schmidt (2006), Global gridded data set of the oxygen isotopic composition in seawater, *Geophys. Res. Lett.*, *33*, L12604, doi:10.1029/2006GL026011.

Levitus, S., J. I. Antonov, T. P. Boyer, and C. Stephens (2000), Warming of the world ocean, *Science*, *287*, 2225–2229, doi:10.1126/science.287.5461.2225.

Lewis, E., and D. W. R. Wallace (1998), Program developed for CO2 system calculations, ORNL/CDIAC-105(Carbon Dioxide Information Analysis Center, Oak Ridge National Laboratory, U.S. Department of Energy, Oak Ridge, Tennessee).

Liu, Z., and M. Alexander (2007), Atmospheric bridge oceanic tunnel and global climatic teleconnections, *Rev. Geophys.*, *45*, RG2005, doi:10.1029/2005RG000172.

Liu, Z., and H. Yang (2003), Extratropical control of tropical climate, the atmospheric bridge and oceanic tunnel, *Geophys. Res. Lett.*, *30*(5), 1230, doi:10.1029/2002GL016492.

Locarnini, R. A., A. V. Mishonov, J. I. Antonov, T. P. Boyer, H. E. Garcia, O. K. Baranova, M. M. Zweng, and D. R. Johnson (2010), *World Ocean Atlas 2009, Volume 1: Temperature*, 184 pp., U.S. Government Printing Office, Washington, D.C.

Lohmann, G. (1995), A model for variation in the chemistry of planktonic foraminifera due to secondary calcification and selective dissolution, *Paleoceanography*, *10*(3), 445–457, doi:10.1029/95PA00059.

Loncaric, N., F. J. C. Peeters, D. Kroon, and G.-J. A. Brummer (2006), Oxygen isotope ecology of recent planktic foraminifera at the central Walvis Ridge (SE Atlantic), *Paleoceanography*, *21*, PA3009, doi:10.1029/2005PA001207.

Lozier, S. M., S. Leadbetter, R. G. Williams, V. Roussenov, M. S. C. Reed, and N. J. Moore (2008), The spatial pattern and mechanisms of heat-content change in the North Atlantic, *Science*, *319*(5864), 800–803, doi:10.1126/science.1146436.

Martínez-Botí, M. A., P. G. Mortyn, D. N. Schmidt, D. Vance, and D. B. Field (2011), Mg/Ca in foraminifera from plankton tows: Evaluation of proxy controls and comparison with core tops, *Earth Planet. Sci. Lett.*, *307*(1-2), 113–125, doi:10.1016/j.epsl.2011.04.019.

Matsumoto, K., and J. Lynch-Stieglitz (2003), Persistence of Gulf Stream separation during the Last Glacial Period: Implications for current separation theories, *J. Geophys. Res.*, *108*(C6), 3174 doi:10.1029/2001JC000861.

Mekik, F., R. François, and M. Soon (2007), A novel approach to dissolution correction of Mg/Ca-based paleothermometry in the tropical Pacific, *Paleoceanography*, *22*, PA3217, doi:10.1029/2007pa001504.

Mix, A. C. (1986), *Late Quaternary Paleoceanography of the Atlantic Ocean: Foraminiferal Faunal and Stable-Isotopic Evidence*, 754 pp., Columbia University, New York.

Mix, A. C., A. E. Morey, N. G. Pisias, and S. W. Hostetler (1999), Foraminiferal faunal estimates of paleotemperature: Circumventing the No-analog problem yields cool Ice Age tropics, *Paleoceanography*, *14*(2), 350–359, doi:10.1029/1999PA900012.

Mohtadi, M., D. W. Oppo, A. Lückge, R. DePol-Holz, S. Steinke, J. Groeneveld, N. Hemme, and D. Hebbeln (2011), Reconstructing the thermal structure of the upper ocean: Insights from planktic foraminifera shell chemistry and alkenones in modern sediments of the tropical eastern Indian Ocean, *Paleoceanography*, *26*, PA3219, doi:10.1029/2011pa002132.

Morard, R., F. Quillévéré, C. J. Douady, C. de Vargas, T. de Garidel-Thoron, and G. Escarguel (2011), Worldwide genotyping in the planktonic foraminifer *Globoconella inflata*: Implications for life history and paleoceanography, *PLoS ONE*, *6*(10), e26,665, doi:10.1371/journal.pone.0026665.

Mortyn, P. G., and C. D. Charles (2003), Planktonic foraminiferal depth habitat and $\delta^{18}O$ calibrations: Plankton tow results from the Atlantic sector of the Southern Ocean, *Paleoceanography*, *18*(2), 1037, doi:10.1029/2001PA000637.

Mulitza, S., A. Dürkoop, W. Hale, G. Wefer, and H. S. Niebler (1997), Planktonic foraminifera as recorders of past surface-water stratification, *Geology*, *25*(4), 335–338, doi:10.1130/0091-7613(1997)025<0335:PFAROP>2.3.CO;2.

Niebler, H. S., H. W. Hubberten, and R. Gersonde (1999), Oxygen isotope values of planktic foraminifera: A tool for the reconstruction of surface water stratification, in *Use of Proxies in Paleoceanography: Examples from South Atlantic*, edited by G. Fisher and G. Wefer, pp. 165–189, Springer, Berlin Heidelberg.

Ortiz, J. D., A. C. Mix, and R. W. Collier (1995), Environmental control of living symbiotic and asymbiotic foraminifera of the California Current, *Paleoceanography*, *10*(6), 987–1009, doi:10.1029/95PA02088.

Quillévéré, F., R. Morard, G. Escarguel, C. J. Douady, Y. Ujiié, T. de Garidel-Thoron, and C. de Vargas (2013), Global scale same-specimen morpho-genetic analysis of *Truncorotalia truncatulinoides*: A perspective on the morphological species concept in planktonic foraminifera, *Palaeogeogr. Palaeoclimatol. Palaeoecol.*, doi:10.1016/j.palaeo.2011.03.013, in press.

Ravelo, A. C., and R. G. Fairbanks (1992), Oxygen isotopic composition of multiple species of planktonic foraminifera: Recorders of the modern photic zone temperature gradient, *Paleoceanography*, *7*(6), 815–831, doi:10.1029/92PA02092.

Regenberg, M., D. Nürnberg, S. Steph, J. Groeneveld, D. Garbe-Schönberg, R. Tiedemann, and W.-C. Dullo (2006), Assessing the effect of dissolution on planktonic foraminiferal Mg/Ca ratios: Evidence from Caribbean core tops, *Geochem. Geophys. Geosyst.*, *7*, Q07P15, doi:10.1029/2005GC001019.

Regenberg, M., S. Steph, D. Nürnberg, R. Tiedemann, and D. Garbe-Schönberg (2009), Calibrating Mg/Ca ratios of multiple planktonic foraminiferal species with δ18O-calcification temperatures: Paleothermometry for the upper water column, *Earth Planet. Sci. Lett.*, *278*(3–4), 324–336, doi:10.1016/j.epsl.2008.12.019.

Reimer, P. J., et al. (2009), INTCAL09 and MARINE09 radiocarbon age calibration curves, 0–50,000 years cal BP, *Radiocarbon*, *51*(4), 1111–1150.

Rickaby, R. E. M., and H. Elderfield (2005), Evidence from the high-latitude North Atlantic for variations in Antarctic intermediate water flow during the last deglaciation, *Geochem. Geophys. Geosyst.*, *6*, Q05001, doi:10.1029/2004gc000858.

Rohling, E. J., and S. Cooke (1999), Stable oxygen and carbon isotopes in foraminiferal carbonate shells, in *Modern Foraminifera*, edited by B. K. Sen Gupta, pp. 239–258, Kluwer Academic Publishers, Dordrecht, The Netherlands.

Rosenthal, Y., and E. A. Boyle (1993), Factors controlling the fluoride content of planktonic foraminifera: An evaluation of its paleoceanographic applicability, *Geochim. Cosmochim. Acta*, *57*(2), 335–346, doi:10.1016/0016-7037(93)90435-Y.

Rosenthal, Y., G. P. Lohmann, K. C. Lohmann, and R. M. Sherrell (2000), Incorporation and preservation of Mg in *Globigerinoides sacculifer*: Implications for reconstructing the temperature and 18O/16O of sea water, *Paleoceanography*, *15*(1), 135–145, doi:10.1029/1999PA000415.

Sadekov, A., S. Eggins, and P. De Deckker (2005), Characterization of Mg/Ca distributions in planktonic foraminifera species by electron microprobe mapping, *Geochem. Geophys. Geosyst.*, *6*, Q12P06, doi:10.1029/2005GC000973.

Savin, S. M., and R. G. Douglas (1973), Stable isotope and magnesium geochemistry of recent planktonic foraminifera from the South Pacific, *Geol. Soc. Am. Bull.*, *84*(7), 2327–2342.

Schiebel, R., and C. Hemleben (2005), Modern planktic foraminifera, *Paläontologische Zeitschrift*, *79*(1), 135–148, doi:10.1007/BF03021758.

Schmidt, G. A., G. R. Bigg, and E. J. Rohlin (1999), Global Seawater Oxygen-18 Database, http://data.giss.nasa.gov/o18data/.

Schott, F. A., J. P. J. McCreary, and G. C. Johnson (2004), Shallow overturning circulations of the tropical-subtropical oceans, in *Earth Climate: The Ocean-Atmosphere Interaction*, Geophysical Monograph Series, vol. 147, edited by C. Wang, S.-P. Xie, and J. A. Carton, pp. 261–304, A. G. Union, Washington D.C.

Shackleton, N. J. (1974), Attainment of isotopic equilibrium between ocean water and benthonic foraminifera genus *Uvigerina*: Isotopic changes in the ocean during the last glacial, paper presented at Les méthodes quantitatives d'étude des variations du climat au cours du Pleistocène, CNRS, Gif sur Yvette.

Simstich, J., M. Sarnthein, and H. Erlenkeuser (2003), Paired $\delta^{18}O$ signals of *Neogloboquadrina pachyderma* (s) and *Turborotalia quinqueloba* show thermal stratification structure in Nordic Seas, *Mar. Micropaleontol.*, *48*, 107–125.

Snowden, D., and R. L. Molinari (2003), Subtropical cells in the Atlantic Ocean: An observational summary, in *Interhemispheric Water Exchange in the Atlantic Ocean*, Elsevier Oceanography Series, vol. 68, edited by G. J. Goni and P. Malanotte-Rizzoli, pp. 287–312, Elsevier, Amsterdam.

Spero, H. J., and D. W. Lea (1996), Experimental determination of stable isotope variability in *Globigerina bulloides*: Implications for paleoceanographic reconstructions, *Mar. Micropaleontol.*, *28*(3-4), 231–246, doi:10.1016/0377-8398(96)00003-5.

Spero, H. J., and D. F. Wiliams (1989), Opening the carbon isotope "vital effect" black box 1. Seasonal temperatures in the euphotic zone, *Paleoceanography*, *4*(6), 593–601, doi:10.1029/PA004i006p00593.

Spero, H. J., J. Bijma, D. W. Lea, and B. E. Bemis (1997), Effect of the seawater carbonate concentration on foraminiferal carbon and oxygen isotopes, *Nature*, *390*, 497–500, doi:10.1038/37333.

Spero, H. J., K. M. Mielke, E. M. Kalve, D. W. Lea, and D. K. Pak (2003), Multispecies approach to reconstructing eastern equatorial Pacific thermocline hydrography during the past 360 kyr, *Paleoceanography*, *18*(1), 1022, doi:10.1029/2002pa000814.

Steph, S., M. Regenberg, R. Tiedemann, S. Mulitza, and D. Nürnberg (2009), Stable isotopes of planktonic foraminifera from tropical Atlantic/Caribbean coretops: Implications for reconstructing upper ocean stratification, *Mar. Micropaleontol.*, *71*(1-2), 1–19, doi:10.1016/j.marmicro.2008.12.004.

Wilke, I., H. Meggers, and T. Bickert (2009), Depth habitats and seasonal distributions of recent planktic foraminifers in the Canary Islands region (29°N) based on oxygen isotopes, *Deep Sea Res., Part I*, *56*(1), 89–106, doi:10.1016/j.dsr.2008.08.001.

Willis, J. K., D. Roemmich, and B. Cornuelle (2004), Interannual variability in upper ocean heat content, temperature, and thermosteric expansion on global scales, *J. Geophys. Res.*, *109*, C12036, doi:10.1029/2003jc002260.

Zhang, D., M. J. McPhaden, and W. E. Johns (2003), Observational evidence for flow between the Subtropical and Tropical Atlantic: The Atlantic subtropical cells, *J. Phys. Oceanogr.*, *33*, 1783–1797, doi:10.1175/2408.1.